Orientational phase transitions in molecular N$_2$ solids: A path-integral Monte Carlo study

M. Presber, D. Löding,[*] and R. Martoňák[†]

Institut für Physik, Johannes-Gutenberg-Universität, D-55099 Mainz, Germany

P. Nielaba[*]

Institut für Physik, Johannes-Gutenberg-Universität, D-55099 Mainz, Germany
and Institut für Theoretische Physik, Universität des Saarlandes, D-66041 Saarbrücken, Germany

A molecular crystal composed of rigid N$_2$ molecules interacting via Lennard-Jones and electrostatic interactions is studied by path-integral Monte Carlo simulations in the constant pressure ensemble. The simulation scheme employed takes fully into account quantum effects on both translational and rotational degrees of freedom of the molecules. The effect of quantum fluctuations on molar volumes, energies, and transition temperatures is studied for different values of the external pressure. At zero pressure the transition temperature from a high-temperature orientationally disordered cubic phase to a low-temperature phase with $Pa3$ structure is reduced by about 11% due to quantum delocalization. With increasing Trotter number, the molar volume and energy at low temperatures approach the experimentally observed values, in contrast to the classical simulations. As the pressure increases, the transition temperature is shifted to larger values and the difference between the classical and quantum values is decreasing. [S0163-1829(98)07238-5]

I. INTRODUCTION

Molecular solids, composed of small or nearly spherical molecules such as H$_2$, N$_2$, C$_{60}$, and C$_{70}$ have received much attention recently.[1–13] In such systems, molecules have translational as well as rotational degrees of freedom. While the molecular centers are fluctuating around stable lattice sites, the molecular axes can orient in various ways with respect to each other and to the underlying lattice, giving rise to a variety of phases distinguished by the orientational order parameter. As this order parameter can change upon varying temperature and pressure, molecular solids often exhibit nontrivial phase diagrams in the T-p plane. It turns out that many of these phase transitions occur at low temperatures and thus quantum effects can be expected to play an important role in the behavior of the system. Since the energy differences between the competing phases are often very low, under particular circumstances the quantum zero-point energy might play even a decisive role in determining the phase stability and therefore the phase diagram of the system, as illustrated by the large isotope effect on the transition pressure observed at the α-γ transition of the nitrogen crystal.[1] A quantitative understanding of the role of quantum effects is therefore desirable. While from experimental studies alone it is hard to assess the relevance of quantum effects at low temperatures quantitatively, computer simulations provide here a convenient tool, allowing the same system to be simulated classically as well as quantum mechanically. Furthermore, provided a good quality potential for the system of interest is available, simulations can have also a predictive power, and yield predictions for the behavior of the system under special conditions, e.g., high pressure, which have not yet been reached experimentally. In general, the role of the quantum effects on the transitions at high pressures is a nontrivial and open question.

In particular, solid N$_2$ exhibits a very rich phase diagram in the T-p plane, which has been extensively studied by experimental, theoretical or simulational techniques. At low temperatures and pressures the system is in the α phase,[4] where the molecular centers of the N$_2$ molecules form a fcc lattice and each molecule of the basis cell is aligned along one of the four cubic body diagonals in such a way that they are perpendicular to each other. With increasing temperature, the system undergoes a phase transition to an orientationally disordered phase. The orientational order-disorder phase transition has been studied by simulational techniques recently.[13–18]

In all these simulational studies, however, the quantum-mechanical nature of the N$_2$ rotors has been neglected. While path-integral Monte Carlo (PIMC) has been successfully applied to study of various crystalline systems, such as argon,[19] polyethylene,[20] and silicon,[21] the distinguishing feature of molecular solids from the point of view of quantum simulations is the presence of the rotational degrees of freedom. These require within a PIMC scheme a special treatment, somewhat different from that applicable to translational degrees of freedom, and it was only recently that a convenient scheme for three-dimensional rotors has been worked out and described in Ref. 22. In this paper we have employed this scheme in a constant pressure PIMC simulation, and applied it to a N$_2$ molecular crystal. We present results for the low-temperature properties, such as molar volume, internal energy and order parameter, and pay particular attention to the study of the phase transition to the orientationally disordered phase at different pressures. We find that in the α phase the molar volume and internal energy at low temperatures are in excellent agreement with experimental values. In order to quantify the amount of quantum effects near the transition temperatures, we also performed some classical simulations. The transition temperature to the high-temperature orientationally disordered phase was found to be reduced by about 11% resulting in a better agreement with the α-β transition temperature obtained by experimental techniques. The ground-state order parameter is reduced by

as much as 20% compared to the classical value. Other quantities, like the volume and order parameter jump at the transition are also calculated and a surprisingly good agreement with experimental data at the α-β transition is found.

The remainder of this article is organized as follows: In Sec. II we describe the model used for nitrogen crystal as well as the path-integral Monte Carlo method for the rotators. In Sec. III we present the simulation results obtained at different pressures and discuss in detail various aspects of the phase transitions observed. We compare our results with experiments for the α phase and for the α-β transition as well as with classical simulations. Finally, in Sec. IV the conclusions are drawn and some further possible directions are suggested.

II. METHOD AND INTERACTION POTENTIALS

A. Interaction potentials

In our studies we model the N_2 molecules as rigid rotors. We specify here the N_2-N_2 interaction potential of the N_2 dimer based on an *ab initio* study.[23] This potential has been modified for high pressures.[27,24,14-17] None of these improved potentials however is capable to successfully describe the presence of all standard N_2 phases found experimentally.[1] Furthermore, the experimentally observed structural fcc-hcp phase transition accompanying the α-β transition has not yet been found by direct simulational techniques using these potentials,[15,17] because of large free-energy barriers between the fcc and the hcp lattice structure.

Here we are mainly interested in the quantifications of quantum effects on the low temperature–low-pressure α phase, and motivated by the success of our previous classical study,[18] we use the unmodified potential derived in Ref. 23, containing the electrostatic interaction potential and the convenient atom-atom Lennard-Jones 6-12 potential.[25,26]

The electrostatic interaction sites are positive charges of magnitude $q_1 = q_2 = 0.373$ e located at distances $\pm$ 1.044 Å away from the molecular center of mass on the molecular symmetry axis and negative charges $q_3 = q_4 = -0.373$ e at distances $\pm$ 0.874 Å, respectively.[27,24,15] The electrostatic interaction $V_{EL}(k,l)$ between the molecules k and l with charges at $\mathbf{r}_{k_m}$ and $\mathbf{r}_{l_n}$ $(m,n = 1,\ldots,4)$ is given by

$$V_{EL}(k,l) = \sum_{m,n=1}^{4} \frac{1}{4\pi\varepsilon_0} \frac{q_m q_n}{|\mathbf{r}_{k_m} - \mathbf{r}_{l_n}|}. \tag{1}$$

B. The path-integral formalism

Having specified the interaction potentials, we can write for our system a full quantum Hamiltonian $\hat{\mathcal{H}}$ which apart from potential energy $\hat{V}_{pot}$ consists of kinetic energy due to translations of the centers of mass, $\hat{T}_{trans}$, and due to molecular rotations $\hat{T}_{rot}$,

$$\hat{\mathcal{H}} = \hat{T}_{trans} + \hat{T}_{rot} + \hat{V}_{pot}. \tag{2}$$

In order to perform path-integral Monte Carlo simulations[28-38,40,41,19,22] we apply the Trotter product for-

mula to the canonical partition function $Z(N,V,T)$ for a system of N particles in the volume V at inverse temperature $\beta = (k_B T)^{-1}$

$$Z(N,V,T) = \mathrm{Tr}(\exp[-\beta\hat{\mathcal{H}}]) \tag{3}$$

and obtain

$$Z(N,V,T) = \lim_{P\to\infty} \mathrm{Tr}(\exp[-\beta\hat{T}_{trans}/P]\exp[-\beta\hat{T}_{rot}/P]$$

$$\times \exp[-\beta\hat{V}_{pot}/P])^P. \tag{4}$$

Here, integer P is the Trotter number. Inserting appropriate complete sets of states, we obtain in coordinate space an expression

$$Z(N,V,T) = \lim_{P\to\infty} \prod_{s=1}^{P} \int d\{\mathbf{r}^{(s)}\} \int d\{\mathbf{n}^{(s)}\}$$

$$\times \exp[-\beta(T_{trans} + T_{rot} + V_{pot})/P], \tag{5}$$

where $\mathbf{r}^{(s)}$ is the vector of a rotator's center of mass at imaginary time slice s and $\mathbf{n}^{(s)}$ the director parallel to the molecular axis, $|\mathbf{n}^{(s)}| = 1$. Due to the cyclic property of the trace periodic boundary conditions have to be applied to the Trotter index, i.e., for $s = P$, $s + 1 = 1$. The full expressions representing the components of the Hamiltonian in Eq. (5) read

$$T_{trans} = T_{trans}(\{\mathbf{r}^{(s)}, \mathbf{r}^{(s+1)}\})$$

$$= \sum_{k=1}^{N} \frac{mP^2}{2\hbar^2\beta^2} (\mathbf{r}_k^{(s)} - \mathbf{r}_k^{(s+1)})^2 - \frac{3NP^2}{2\beta} \ln\frac{mP}{2\pi\hbar^2\beta}, \tag{6}$$

$$T_{rot} = T_{rot}(\{\mathbf{n}^{(s)}, \mathbf{n}^{(s+1)}\})$$

$$= \sum_{k=1}^{N} \sum_{L=0}^{\infty} \left[BL(L+1) + \frac{P}{\beta}\ln\frac{2L+1}{4\pi} P_L(\mathbf{n}_k^{(s)} \cdot \mathbf{n}_k^{(s+1)}) \right], \tag{7}$$

$$V_{pot} = V_{pot}(\{\mathbf{r}^{(s)}, \mathbf{n}^{(s)}\}) = V_{LJ}(\{\mathbf{r}^{(s)}, \mathbf{n}^{(s)}\}) + V_{EL}(\{\mathbf{r}^{(s)}, \mathbf{n}^{(s)}\}), \tag{8}$$

where P_L denotes the Legendre polynomial. For N_2 rotators, the mass m and the rotational constant B are equal to $m = 28.02$ u and $B = 2.88$ K, respectively.

The nuclear spin of the N atom is 1, thus for the N_2 molecule two variants have to be considered: *ortho*-N_2 and *para*-N_2, for the former the nuclear spins are parallel, for the latter antiparallel. The total wave function of the bosonic N_2 molecule, consisting of the total nuclear spin times the rotational state, has to be symmetric under intramolecular exchange of the atoms, which means that only the combinations of antisymmetric spin functions times odd rotational levels or of symmetric spin functions times even rotational levels have to be considered. As a consequence, for *ortho*-N_2 only the even L values in Eq. (7) appear, for *para*-N_2 only the odd L values. This principal distinction of the different variants of the N_2 molecule however are only important at low temperatures. In Ref. 22 the propagator for an orientational degree of freedom, $K_{s,s+1}(N=1) = \exp[-\beta T_{rot}(N$
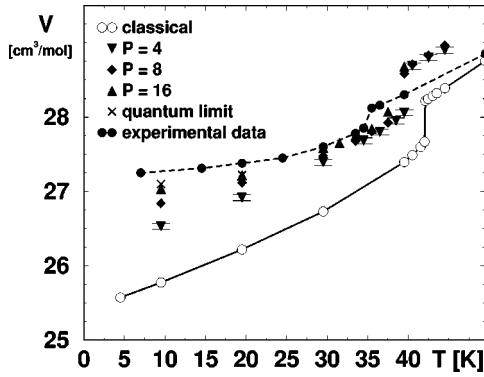
FIG. 1. Equilibrium volume versus temperature at zero pressure. Simulation results for various Trotter dimensions P as indicated in the figure, the results for $P=1$ correspond to a classical simulation, lines are for visual help. The data connected by dashed lines are the experimental volumes near the transition (Ref. 11) from the $Pa3$ to the β structure. Errors for simulation results are equal (PIMC) or smaller (classical MC) than symbol sizes.

$=1)/P]$, has been studied for the three different cases, full summation over all L values (even and odd), summation over even L and summation over odd L values. For temperatures and P values, for which $\beta B/P<0.1$, $K_{s,s+1}(N=1)$ does not show any visible differences for these cases for angles $\gamma_s = \arccos[\mathbf{n}^{(s)}\cdot\mathbf{n}^{(s+1)}]<\pi/2$. Since the N_2 molecule is a relatively heavy molecule, at temperatures above 5 K the molecule is quite well localized (compared to H_2 molecules) and so the angle differences between neighboring ''Trotter'' slices s and $s+1$ are small. This means that for $T>5$ K only small γ values are important in the Metropolis step, independent on the *ortho/para* variant of the N_2 molecule. This finding is in agreement with the results of Ref. 42, where it was found that the differences between *ortho*- and *para*-N_2 molecules adsorbed on graphite are negligible for temperatures above 5 K. The general consideration of Ref. 39 shows that in general the influence of the quantum statistics vanishes for temperatures exceeding five times the rotational constants.[39] According to Ref. 1 the energy difference between the ortho and para levels of solid α nitrogen can be estimated to be in the order of one microdegree. As our simulations are performed above 10 K, these results motivated us to neglect the *ortho/para* distinction and to perform the simulations with a propagator consisting of the summation over even L values in Eq. (7). The interaction potential V_{pot} for particles at the same imaginary time slice s consists of a Lennard-Jones and an electrostatic interaction as specified in the previous subsection.

We performed our simulation in the NpT ensemble at constant external pressure p. In this ensemble the partition function $Z_p(N,p,T)$ reads

$$Z_p(N,p,T)=\int_0^\infty dV e^{-\beta pV}\ Z(N,V,T). \qquad (9)$$

In the simulation a symmetrical deformation tensor h is introduced allowing volume changes as well as changes of the box shape, for details of the technique employed see Ref. 18. Periodic boundary conditions have been applied in all spatial directions.
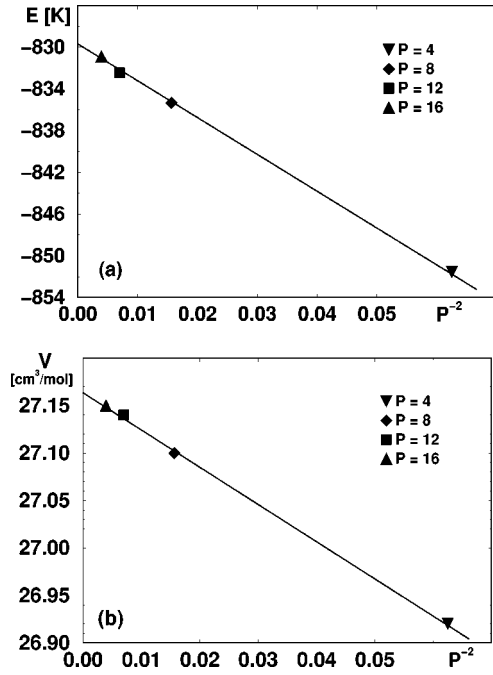

FIG. 2. Trotter scaling plots of the molecular energy (a) and molar volume (b) at zero pressure and temperature $T=20$ K. Points are PIMC results, the lines are the extrapolation lines to the Trotter limit ($P\to\infty$). Errors are smaller than symbol sizes.

Averages $\langle A\rangle$ of observables A for a fixed value of the Trotter index P can be obtained with the standard measures given by the Boltzmann factors in Eqs. (4) and (8). Beside the kinetic and potential energies and the equilibrium volume we determine the orientational order parameter Q as a function of temperature. Q is the average of the order parameters Q_X being defined for each sublattice $X=1,\ldots,4$ of the $Pa3$ phase according to

$$Q_X=\frac{3}{2}\frac{1}{P}\sum_{s=1}^{P}\sum_{\mu,\nu=1}^{3}\left\langle\left(\sum_{k\epsilon X}\left[n_k^{\mu(s)}n_k^{\nu(s)}-\frac{\delta_{\mu\nu}}{3}\right]\right)^2\right\rangle. \quad (10)$$

Here $n_k^{\mu(s)}$ is the μth component of the director $\mathbf{n}_k^{(s)}$ of the kth molecule at time slice s.

In the simulation a Monte Carlo step consists of N attempted random displacements of the centers of masses as well as of the centers of the angles, and of NP attempted random displacements of coordinates and angles at the imaginary time slices, see Eqs. (5) and (6), as well as of a volume deformation attempt, where the maximum displacements are fixed by the 50% acceptance rule. In most of our simulations we chose the number of N_2 molecules as $N=500$ (i.e., five unit cells in each direction), the Trotter dimension was chosen such that the quantum limit was reached within numerical scatter. It turned out that a value of $P=8$ was sufficient for computations at temperatures close to the phase-transition temperature. A typical run with 10^4 Monte Carlo steps took about 75 CPU hours on a CRAY-T3E (single processor), 12 CPU hours on a CRAY-YMP and 5 CPU hours on a CRAY-T90; in total the present study required CPU time equivalent to 600 CPU hours on a CRAY-T90.
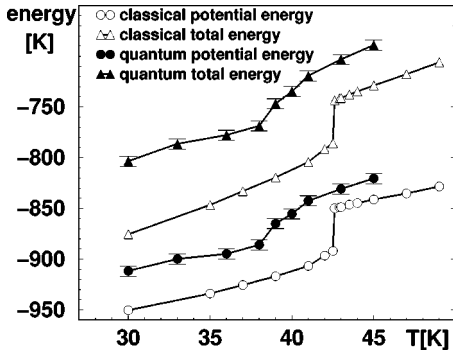
FIG. 3. Classical and quantum energies as functions of temperature at zero pressure. Points are simulation results ($P=8$ for the PIMC simulations), lines are for visual help. Error bars of classical results are smaller than symbol sizes.
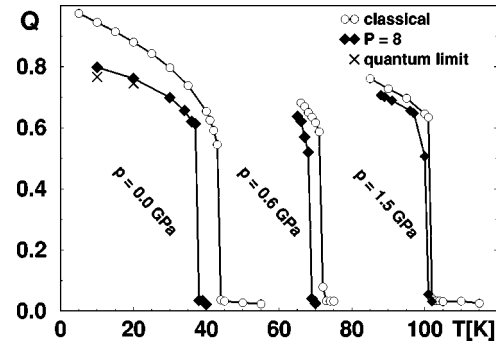

FIG. 4. Order parameter as function of temperature for various pressures. Points are simulation results [classical MC and PIMC ($P=8$) results], lines are for visual help, error bars are smaller than symbol sizes.

III. RESULTS AND DISCUSSION

At first we present the results and discuss the case of zero external pressure. In Fig. 1 the temperature dependence of the molar volume is shown for our simulational as well as for experimental data.[11] Direct comparison between simulation and experiment is only possible for the low-temperature α phase up to the phase transition. In the high-temperature disordered phase a direct comparison of the experimental molar volume to both classical and quantum results is, however, not possible here, since the simulation technique used is not able to reproduce the experimentally observed crystal structure above the transition temperature (Sec. II A). Both classical and quantum simulation results are shown in this region, although the difference between the classical and quantum value of the molar volume is considerably smaller compared to the low-temperature ordered phase and we stress that their relation to the experimental molar volume, in particular the fact that the classical values appear to be closer to the experiment than the quantum ones, has to be regarded as accidental. In this work we aimed at a pioneering study on the quantification of the quantum effects in the α phase and on the orientational phase transition from the α phase to the orientationally disordered fcc phase. So the high-temperature values of the simulation (disordered fcc) cannot be compared to the experimental data (hcp).

In Fig. 1 we note that the classical simulations (corresponding to $P=1$) lead to a nonzero slope of the volume at very low temperatures which is in sharp contrast to the experimental behavior.[11] With increasing values of P the molar

volume obtained from the present simulation is in a progressively better agreement with the experimental values. A typical Trotter-scaling plot of the molar volume and the energy per molecule shows the approach of the observables to the asymptotic P^{-2} dependency, see Fig. 2. Standard Trotter-scaling extrapolation techniques to the quantum limit finally result in low-temperature molar volume values which are in excellent agreement with the experiment, see Fig. 1. The energy as function of temperature is shown in Fig. 3. We note that at $T \approx 30$ K the potential energy in the quantum simulation is enhanced by about 40 K compared to the classical case due to quantum fluctuations. The kinetic energy, consisting of rotational and translational energy is larger than the classical value, see Table I, and approaches the classical equipartition value $(5/2)k_BT$ at high temperatures. From the PIMC simulation results for the energies we conclude that the ground-state energy per molecule is about -830 K, which is in good agreement with experimental values for the sublimation energy (-833 K),[1] in contrast to the results of a classical simulation, see Fig. 3.

Upon heating a phase transition takes place from the α phase to an orientationally disordered fcc phase at the transition temperature T_1, where we find a jump in the molar volume (Fig. 1), the molecular energy (Fig. 3), and in the order parameter Q (Fig. 4). Upon cooling the phase transition from the orientationally disordered fcc phase to the α phase is at a temperature T_2, which is at most 2 K below T_1, such that the hysteresis range at the transition is smaller than 2 K. Since the transition temperatures presented in this study are thus determined with an accuracy of less than 1 K, we did

TABLE I. Comparison of quantum rotational and quantum translational energy with the predictions of the classical equipartion theorem ($p=0.0$ GPa, $P=8$, $k_B=1$).

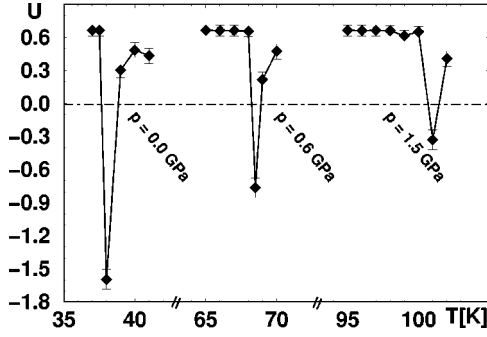| T (K)	$E_{\rm rot}^{qm}$ (± 1) (K)	$E_{\rm rot}^{cl}=\frac{2}{2}k_BT$ (K)	$E_{\rm trans}^{qm}$ (± 1) (K)	$E_{\rm trans}^{cl}=\frac{3}{2}k_BT$ (K)
20	37.2	20	57.8	30.0
37	46.9	37	74.0	55.5
38	47.1	38	72.3	57.0
39	44.7	39	71.3	58.5
40	42.4	40	73.6	60.0
41	44.3	41	73.1	61.5
45	48.4	45	80.5	67.5
70	72.2	70	110.1	105.0

FIG. 5. Fourth-order cumulant of the order parameter as function of temperature for various pressures. Points are PIMC simulation results ($P=8$), lines are for visual help.

FIG. 6. Phase transitions from the α phase to the orientationally disordered fcc phase (simulation), classical (open spheres), and quantum results (diamonds, lines are for visual help). The experimental transition from the high temperature β phase to the low-temperature phases with orientational order is shown for comparison by a line, α-β: from Ref. 47, γ-β: from Ref. 48. Experimentally there is a transition between the low-pressure α and high-pressure γ phase, which is not shown here for the sake of clarity.

not try to reduce this small temperature range further by determining free-energy intersection points. We note however, that in other studies[15] large ''hysteresis'' regions have been found when the transition from the α phase to the orientationally disordered fcc phase upon heating has been compared to the transition from the orientationally disordered hcp phase to the orientationally ordered hcp phase upon cooling. We are not yet interested in quantifying the α-β transition temperature because of the above-mentioned general problems to simulate structural phase transitions by direct methods.

Many details concerning the orientational phase transition studied here involve changes in thermodynamic properties which are in good agreement with those found in the experimental α-β transition. We thus find it appropriate to compare the numerical values of these quantities. The transition temperature of our previous classical Monte Carlo study[18] is $T_1=42.5$ (± 0.3) K and the volume change $\Delta V=0.55$ (± 0.03) cm^3/mol, see Fig. 1. With increasing Trotter number the transition temperature is shifted to smaller values, and in the quantum limit we obtain $T_1^{qm}=38$ (± 0.5) K, which represents a reduction of about 11% with respect to the classical value. The experimental value[11] is $T_1^{exp} \approx 35$ K. As we only study the orientational transition to the disordered fcc lattice, a better agreement with the experimental value at the α-β transition can hardly be expected. The same holds for the obtained volume change at the transition, $\Delta V^{qm}=0.6$ (± 0.05) cm^3/mol which remains higher than the experimental volume change $\Delta V^{exp} \approx 0.3$ cm^3/mol. At the transition the total energy increases by about $\Delta E=45$ (± 5) K. On the contrary to the potential and the translational energy, the rotational energy decreases at the transition, see Table I. This behavior is due to the fact that the rotational constraints in the low-temperature phase with ori-
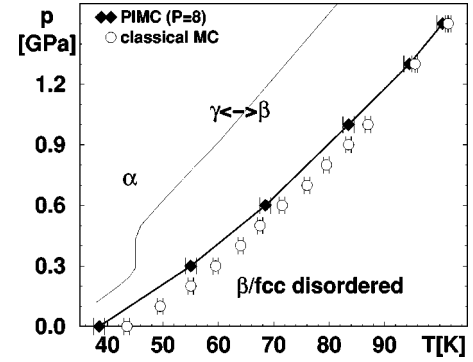
entational order are removed in the disordered phase, which results in a lowering of the rotational energy.

The PIMC value of the order parameter at low temperatures is reduced by about 20% compared to the classical value of 1, see Fig. 4, due to ground-state fluctuations of the rotors around their potential minima. At the phase transition the jump in the order parameter is in good agreement with experiment; both experiment[43] and simulation show a jump of the order of $\Delta Q=0.6$. Quantum delocalization leads to a smaller order parameter and thus to a smaller ΔQ; the lower transition temperature, on the other hand, reduces thermal fluctuations, resulting in a larger value of ΔQ. These combined effects results in essentially the same value for ΔQ in the quantum and the classical computation, see Fig. 4.

The classification of the transition as first order can be justified by observing the jumps in volume and energy at the transition temperature or by the fourth-order cumulant[44,45] $U(T)$ of the order parameter:

$$U(T)=1-\frac{1}{3}\frac{\langle Q^4 \rangle}{\langle Q^2 \rangle^2}.\qquad (11)$$

$U(T)$ approaches the value of 2/3 in the ordered low-temperature phase and in the case of a second-order transition monotonically decreases with increasing temperature. In the case of a first-order transition $U(T)$ has a pronounced minimum with negative values for temperatures slightly above the transition temperature.[46] In Fig. 5 the cumulant is

TABLE II. Difference in the molar volume (PIMC), the total energy (PIMC), and the order parameter (PIMC and MC) between the two phases at the orientational phase transition.

p (GPa)	ΔV^{qm} (± 0.05) (cm^3/mol)	ΔE^{qm} (± 5) (K])	$\Delta Q^{qm}(\pm 0.03)$	$\Delta Q^{cl}(\pm 0.02)$
0.0	0.6	45	0.53	0.59
0.3	0.5	48	0.50	0.59
0.6	0.3	46	0.49	0.60
1.0	0.2	41	0.53	0.62
1.5	0.2	43	0.49	0.58

TABLE III. Left- and right-hand side of Eq. (12) for different pressures.

p (GPa)	$\Delta E(\pm 5)$ (K)	$p\Delta V (\pm 6)$ (K)	$\lambda = \Delta E + p\Delta V$ (± 8) (K)	$T\Delta V(dp/dT)$ (± 6) (K)
0.0	45	0	45	51
0.3	48	18	66	74
0.6	46	22	68	66
1.0	41	24	65	59
1.5	43	36	79	71

shown and we find this characteristic of a first-order transition.

We have studied the phase transition also for higher external pressures and the resulting phase diagram in the pressure-temperature plane is shown in Fig. 6. As already mentioned at the beginning of this section, a comparison of simulation results with experimental data is only possible for the low-temperature α phase. With increasing pressure the transition temperature is shifted to higher values and the difference between the classical and the quantum transition temperatures decreases. The reason for this behavior is that at higher pressures the particle distances become smaller and the effective potential acting on one particle is more structured which results in a sharper localization of the rotators. As a consequence, the transition temperature is increased, and the effect of quantum fluctuations is correspondingly reduced. We note again here that at higher pressures the question of appropriate potential is still open and our main concern at this point was the investigation of quantum effects for a given potential rather than reproducing the actual experimental phase boundary.

In Figs. 4 and 5 we show Q and $U(T)$ for different pressures as functions of the temperature. As in the case of zero pressure, $U(T)$ shows a pronounced minimum at the transition, ΔQ apparently does not depend strongly on the pressure. In Table II we show the volume jump ΔV at the transition as a function of the pressure. We note that ΔV is decreasing with increasing pressure and seems to approach a limiting value of about 0.2 cm^3/mol for large pressures.

The Clausius-Clapeyron equation describes the thermodynamics of such a first-order phase transition:

$$\lambda = T\Delta V \frac{dp}{dT}. \qquad (12)$$

Here λ is the change in enthalpy at the transition, or the latent heat: $\lambda = \Delta E + p\Delta V$. In Table III we compare both sides of Eq. (12) computed with PIMC results for ΔV and ΔE and taking numerically the derivative of the (PIMC) transition pressure with respect to the temperature. We find good agreement within numerical accuracy, indicating that the pressure dependency of λ is mainly due to the $p\Delta V$ term, which may explain why the energy jump ΔE at the transition is quite independent on the pressure (see Table II).

IV. SUMMARY AND CONCLUSION

In this paper a detailed study of phase transitions in molecular N_2 solids by path-integral Monte Carlo simulation methods was presented. Assuming a model representing the intermolecular interactions by Lennard-Jones and Coulomb potentials and allowing for quantum effects on both translational and rotational degrees of freedom to be taken into account we found that the quantum results for the molar volume and the internal energy in the low-temperature α phase are in good agreement with experimental values.

The transition temperature from the orientationally ordered fcc solid to the high-temperature disordered fcc solid is reduced by about 11% at zero pressure due to quantum delocalization effects which weaken the orientational order compared to the classical case. The quantum transition temperature is now much closer to the experimental value for the α-β transition. Within this approach a better agreement can hardly be expected, since the orientational order-disorder transition in the experiment is accompanied by a structural phase transition from the fcc to the hcp lattice. The ground-state order parameter is actually reduced by as much as 20% compared to the classical value.

With increasing pressure the transition temperature is shifted to larger values. At these higher temperatures the quantum effects are weakened and thus the difference between the classical and the quantum transition temperature is decreasing with increasing pressure.

Our results show that the quantum effects on the phase transitions are important at low temperatures and cannot be neglected in theoretical studies. This may also shed a new light on procedures where interaction potentials are designed by fitting classical results to experimental findings.

In future work we intend to use similar methods to quantify the quantum effect on other phase transitions in N_2 solids as well as in solids constituting of mixtures of N_2 molecules and Ar atoms. In this context, the α-γ transition in N_2 and the associated pronounced isotope effect represent an interesting challenge to be studied by quantum simulation techniques. We believe that methods analogous to those used in this paper would be applicable also to study other molecular solid state systems, of which the solid phase of hydrogen are of particular interest.[49]

*Permanant address: Fakultät für Physik, Universität Konstanz, D-78457 Konstanz, Germany.

†Permanent address: Department of Physics, Faculty of Electrical Engineering, Slovak Technical University, Ilkovičova 3, 812 19 Bratislava, Slovakia.

[1] T.A. Scott, Phys. Rep. **27**, 901 (1976).

[2] R. Sachidanandam and A.B. Harris, Phys. Rev. Lett. **67**, 1467 (1991).

[3] W.I.F. David, R.M. Ibberson, J.C. Matthewman, K. Prassides, T.J.S. Dennis, J.P. Hare, H.W. Kroto, R. Taylor, and D.R.M. Walton, Nature (London) **353**, 147 (1991).

[4] J.A. Venables and C.A. English, Acta Crystallogr., Sect. B: Struct. Crystallogr. Cryst. Chem. **30**, 929 (1974).

[5] M. Sprik, A. Cheng, and M.L. Klein, Phys. Rev. Lett. **69**, 1660 (1992).

[6] G. Van Tendeloo, S. Amelinckx, J.L. de Boer, S. van Smaalen, M.A. Verheijen, H. Meeks, and G. Meijer, Europhys. Lett. **21**, 329 (1993).

[7] K. Knorr and A. Loidl, Phys. Rev. B **31**, 5387 (1993).

[8] S. Elschner, K. Knorr, and A. Loidl, Z. Phys. B **61**, 209 (1985).

[9] D. Lamoen and K.H. Michel, J. Chem. Phys. **101**, 1435 (1994); K.H. Michel, D. Lamoen, and W.I.F. David, Acta Crystallogr., Sect. A: Found. Crystallogr. **A51**, 365 (1995).

[10] A.K. Callebaut and K.H. Michel, Phys. Rev. B **52**, 15 279 (1995).

[11] H. Klee and K. Knorr, Phys. Rev. B **42**, 3152 (1990).

[12] M.H. Müser, J. Phys.: Condens. Matter **8**, 913 (1996).

[13] S. Raugei, G. Cardini, V. Schettino, and H.J. Jodl, J. Chem. Phys. **106**, 8196 (1997).

[14] J. Belak, R. Le Sar, and R.D. Etters, J. Chem. Phys. **92**, 5430 (1990).

[15] B. Kuchta, K. Rohleder, R.D. Etters, and J. Belak, J. Chem. Phys. **102**, 3349 (1995).

[16] A. Mulder, J.P.J. Michels, and J.A. Schouten, J. Chem. Phys. **105**, 3235 (1996).

[17] A. Mulder, J.P.J. Michels, and J.A. Schouten, J. Chem. Phys. **106**, 8806 (1997).

[18] D. Löding, M.H. Müser, and P. Nielaba, Z. Phys. B **102**, 505 (1997).

[19] M.H. Müser, P. Nielaba, and K. Binder, Phys. Rev. B **51**, 2723 (1995).

[20] R. Martoňák, W. Paul, and K. Binder, Phys. Rev. E **57**, 2425 (1998).

[21] C. Rickwardt and P. Nielaba (unpublished).

[22] M.H. Müser, Mol. Simul. **17**, 131 (1996).

[23] R.M. Berens and A. van der Avoird, J. Chem. Phys. **72**, 6107 (1980).

[24] J. Belak, R. Le Sar, and R.D. Etters, J. Chem. Phys. **89**, 1625 (1988).

[25] P.S.Y. Cheung and J.G. Powles, Mol. Phys. **30**, 921 (1975).

[26] The Lennard-Jones parameters of nitrogen are $\varepsilon_{NN}=0.515 \times 10^{-21}$ J and $\sigma_{NN}=3.310$ Å are located at a distance $d = 0.547$ Å away from the molecular center of mass. Interactions up to the fourth-neighbor shell were taken into account, the next-neighbor shells (5–20) have been treated in a static lattice approximation, the rest in a continuum static approximation.

[27] R.D. Etters, V. Chandrasekharan, E. Uzan, and K. Kobashi, Phys. Rev. B **33**, 8615 (1986).

[28] R.P. Feynman and A.R. Hibbs, *Quantum Mechanics and Path Integrals* (McGraw-Hill, New York, 1965); H.F. Trotter, Proc. Am. Math. Soc. **10**, 545 (1959); M. Suzuki, Prog. Theor. Phys. **46**, 1337 (1971); Commun. Math. Phys. **51**, 183 (1976); L.S. Schulman, *Techniques and Applications of Path Integration* (Wiley, New York, 1981); H. Kleinert, *Path Integrals in Quantum Mechanics, Statistics and Polymer Physics* (World Scientific, Singapore, 1990).

[29] J.A. Barker, J. Chem. Phys. **70**, 2914 (1979); K.S. Schweizer, R. M. Stratt, D. Chandler, and P.G. Wolynes, *ibid.* **75**, 1347 (1981); D. Chandler and P.G. Wolynes, *ibid.* **74**, 4078 (1981).

[30] B.J. Berne and D. Thirumalai, Annu. Rev. Phys. Chem. **37**, 401 (1986); *Quantum Monte Carlo Methods*, edited by M. Suzuki, Springer Series in Solid State Sciences, Vol. 74 (Springer, New York, 1987); *Quantum Simulation of Condensed Matter Phenomena*, edited by J.D. Doll and J.E. Gubernatis (World Scientific, Singapore, 1990); K.E. Schmidt and D.M. Ceperley, in *The Monte Carlo Method in Condensed Matter Physics*, Topics in Applied Physics Vol. 71, edited by K. Binder (Springer, Berlin, 1992); M.J. Gillan, in *Computer Modelling of Fluids, Polymers and Solids*, edited by C.R.A. Catlow, S.C. Parker, and M.P. Allen (Kluwer, Dordrecht, 1990); D. Chandler, in *Liquids, Freezing and Glass Transition*, edited by J. P. Hansen, D. Levesque, and J. Zinn–Justin (Elsevier, Amsterdam, 1991); D. M. Ceperley, Rev. Mod. Phys. **67**, 279 (1995); P. Nielaba, in *Annual Reviews of Computational Physics V*, edited by D. Stauffer (World Scientific, Singapore, 1997), p. 137.

[31] M.H. Müser, W. Helbing, P. Nielaba, and K. Binder, Phys. Rev. E **49**, 3956 (1994).

[32] M. Kreer and P. Nielaba, in *Monte Carlo and Molecular Dynamics of Condensed Matter Systems*, edited by K. Binder and G. Ciccotti (SIF, Bologna, 1996), p. 501.

[33] D. Marx and P. Nielaba, J. Chem. Phys. **102**, 4538 (1995).

[34] R. Martoňák, D. Marx, and P. Nielaba, Phys. Rev. E **55**, 2184 (1997).

[35] D. Marx and P. Nielaba, Phys. Rev. A **45**, 8968 (1992).

[36] M.H. Müser and B.J. Berne, Phys. Rev. Lett. **77**, 2638 (1996).

[37] D. Marx, Mol. Simul. **12**, 33 (1994).

[38] K.J. Runge, M.P. Surh, C. Mailhiot, and E.L. Pollock, Phys. Rev. Lett. **69**, 3527 (1992).

[39] D.A. McQuarrie, *Statistical Mechanics* (Harper Collins, New York, 1976), Chap. 6-5.

[40] D. Marx, O. Opitz, P. Nielaba, and K. Binder, Phys. Rev. Lett. **70**, 2908 (1993).

[41] J. Cao, Phys. Rev. E **49**, 882 (1994).

[42] D. Marx, S. Sengupta, and P. Nielaba, J. Chem. Phys. **99**, 6031 (1993).

[43] H. Klee and K. Knorr, Phys. Rev. B **43**, 8658 (1991).

[44] K. Binder, Z. Phys. B **43**, 119 (1981); Phys. Rev. Lett. **47**, 693 (1981).

[45] K. Binder, Ferroelectrics **73**, 43 (1987).

[46] K. Vollmayr, J.D. Reger, M. Scheucher, and K. Binder, Z. Phys. B **91**, 113 (1993).

[47] J.R. Brookeman and T.A. Scott, J. Low Temp. Phys. **21**, 491 (1973).

[48] J.W. Steward, J. Phys. Chem. Solids **1**, 146 (1956).

[49] F. Moshary, N.H. Chen, and I.F. Silvera, Phys. Rev. Lett. **71**, 3814 (1993).